

## **Contents:**

Text S1: Method to fix phase offsets in the 2012 data

Text S2: PSD plots for 2012 and 2015

Text S3: Tide and tidal rate

Text S4: Phase lag maps for K1 and S2 tidal frequencies

Text S5: Geometry between velocity and radar LOS

Text S6: Movies shown major calving (-like) events during 3 campaigns

Figure and movie contents are introduced in the text.

## 1. Method to fix phase offsets in the 2012 data

Ice velocity estimates have some significant offsets in the 2012 data. These offsets represent phase discontinuities, clustering at integer multiples of the radar wavelength (Fig. S1(a)). They occur because the 2012 data were acquired with a scan rate that was slow compared to ice velocity, such that ice could move more than one radar wavelength relative to adjacent area during the 3 minute scan interval (data in later years were acquired with a faster scan rate). Compared to fast moving ice, rocks near the TRI can be treated as stationary objects. We used a rock reference point ~0.2 km away from the radar as a reference for phase unwrapping. To correct the phase discontinuities caused by phase unwrapping error, we firstly used a model to fix the phase offsets for a single point on ice (P0, yellow point in Fig. S1(b)), then used it as reference point for phase unwrapping to get velocity maps relative to this point. Ice velocities relative to the stationary rock were then generated by adding the modeled velocities of P0 to those relative velocities. We selected data obtained between 6 August and 10 August for the following process because there were continuous measurements during this period and only one small calving event. Here are the 4 steps used to model the velocity of P0:

- 1) Use the same data processing procedure as described in *Voytenko et al.* [2015]) and *Xie et al.* [2016], generating time series for all velocity maps. The generated velocities are absolute velocities, plus/minus some value equal to an integer number of wavelength jumps. The TRI instrument transmits Ku-band microwaves with wavelength of 1.74 cm. In a 2-way measurement system, 1 wavelength jump in unwrapped phase leads to 0.87 cm change in the LOS displacement, equal to  $4.2 \text{ m d}^{-1}$  offset in LOS velocity when the repeating time of measurement is 3 minutes. From Fig. S1(a) we infer that most of the unwrapped phases for P0 have 4 cycles of phase offset.

- 2) Remove “apparent outliers” by using the modified Z-score method [*Iglewicz and Hoaglin*, 1993]. For the  $i$ th observation  $x_i$ , its Z-score is:

$$Z_i = 0.6745(x_i - \tilde{x}) / \text{MAD} \quad (\text{S1})$$

where MAD denotes the median absolute deviation, and  $\tilde{x}$  is the median value. Observations with absolute value of the modified Z-scores  $>3.5$  were considered as outliers and removed. Then we subtracted a 2nd-order polynomial curve to remove the possible response to calving events. The method by *Davis et al.* [2014] was then used to estimate the periodic components caused by tidal variations. We chose 3 sinusoids with the same frequencies as the K1/M2/S2 tidal constituents (see the main paper for more information about the tidal constituents at Jakobshavn Isbræ). The solid blue curve in Fig. S1(c) shows the best fit of a 2nd-order polynomial plus 3 sinusoids to the observed time series. The dashed blue curves mark 3 times the value of the root-mean-square (RMS) of the residuals.

- 3) Shift all observations (including “apparent outliers” in step 2) upwards/downwards by  $4.2 \times N \text{ m d}^{-1}$ , where  $N = 0, \pm 1, \pm 2, \pm 3, \pm 4, \pm 5$ , etc. Observations who’s shifted values do not fall into the  $3 \times \text{RMS}$  space defined in step 2 are labeled as outliers (grey dots in Fig. S1(c)) and removed. Values that fall within the  $3 \times \text{RMS}$  space are then shifted by 4 cycles of phase offset ( $16.8 \text{ m d}^{-1}$ ) to eliminate the jumps derived by feature tracking method in

step 1.

- 4) Apply a median filter (kernel size = 3) to the time series from step 3, and then use the same model in step 2 to fit the new time series. Estimated parameters are then used for further processing. Fig. S1(d) shows the least square fit of the final fixed time series for P0.

For all other points on the TRI image, their velocities are estimated by adding the modeled velocity of P0 to their relative velocities. Fig. S2 shows phase offsets-fixed LOS velocities for selected points. Black dots are velocity estimates when using a stationary rock point as the reference point for phase unwrapping (shifted upwards by 4 cycles of phase offsets). From Fig. S2 we see that phase jumps are greatly reduced by this method, especially on the glacier. In the mélange, time series shortly after two calving events (on 5 August and 9 August, see blue arrows in Fig. S1(a)) still have some jumps, mainly due to phase breaks caused by rapid ice motion after calving events. In the tidal analysis section of the main paper, we omit data for the mélange acquired near these 2 calving events.

We used feature tracking (done with OpenCV: <http://opencv.org/>) as an independent method to examine the phase offset “fixed” velocities from interferometry. And used stationary or near-stationary points near the radar as references to calculate uncertainties in feature tracking, which is  $<1 \text{ m d}^{-1}$  in both x and y components for velocity estimates based on a TRI intensity image pair separated by 1 day. Fig. S3(a) is the median LOS velocity map from a 1 day sequential measurements in the 2012 campaign. Fig. S3(b) shows a velocity map (projected onto the LOS direction) derived by feature tracking using two TRI intensity images acquired at the beginning and end of the day (red means moving towards the radar, yellow means moving away). Fig. S3(c) is the difference between (a) and (b). Red means the velocity estimated by interferometry is larger than the velocity estimated by feature tracking, yellow means it is less. For most points, the difference is much smaller than 1 cycle of phase jump ( $4.2 \text{ m d}^{-1}$ ). On the north edge of the mélange, there is a small area where offsets still exist, presumably caused by phase breaks due to discontinuities in the TRI maps. One way to solve this type of phase jump is to use shorter repeat time when collecting data. However, this problem won't affect the following tidal analysis if the sign of LOS velocity has not been changed by these phase jumps. Because this study focuses on short time-scale tidal responses, the large background velocity was detrended before tidal analysis. We also noticed that the velocity differences near the radar are much larger, up to a few cycles of phase jumps. This is due to the fact that the phase data for stationary areas near the radar have no discontinuity problems in speed as on the ice. The method described above has thus introduced some artificial jumps in the stationary near field.

Fig. S4 and S5 show comparisons of velocity estimates by interferometry and feature tracking for 2015 and 2016. There are no systematic differences for these two years. Except for some random errors, significant differences only appear in isolated patches where the phase map lacks continuity, or in places close to where calving events have occurred. Thus, we did not apply the same method used for 2012 to the 2015 and 2016 data. Instead, we did phase

unwrapping by using stationary points on rocks only.

## 2. PSD plots for 2012 and 2015

Fig. S6, power spectral density (PSD) for selected areas in 2012

Fig. S7, power spectral density (PSD) for selected areas in 2015

## 3. Tide and tidal rate

Fig. S8 shows predicted and observed tide and tidal rate during 2015 campaign. In this study, tidal rate is defined as the 1st time derivative of tidal height. For a tide signal:

$$H(t) = A \cos(2\pi ft + \varphi) \quad (S2)$$

where  $A$  is the amplitude,  $f$  is the frequency,  $\varphi$  is the phase. The tidal rate is:

$$H'(t) = 2\pi f A \cos(2\pi ft + \varphi + 0.5\pi) \quad (S3)$$

Compare to tidal height, the amplitude of tidal rate has been amplified by  $2\pi f$ . Due to differentiation, the phase difference between ice velocity and tidal rate is the same as the phase difference between ice position and tidal height.

## 4. Phase lag maps for K1 and S2 tidal frequencies

Fig. S9, phase lag in time (h) for K1 and S2 tidal frequencies.

## 5. Geometry between velocity and radar LOS

Fig. S10, geometry used to project velocity onto radar LOS direction.

## 6. Movies shown major calving event during 3 campaigns

Mov. S1, Major calving events in 2012.

Mov. S2, Major calving events in 2015.

Mov. S3, Major calving (-like) events in 2016.

## References

- An, L., Rignot, E., Elieff, S., Morlighem, M., Millan, R., Mouginot, J., Holland, D.M., Holland, D. and Paden, J.: Bed elevation of Jakobshavn Isbræ, West Greenland, from high-resolution airborne gravity and other data, *Geophys. Res. Lett.*, 44(8), 3728–3736, doi: 10.1002/2017GL073245, 2017.
- Davis, J.L., De Juan, J., Nettles, M., Elosegui, P. and Andersen, M.L.: Evidence for non-tidal diurnal velocity variations of Helheim Glacier, 15 East Greenland, *J. Glaciol.*, 60(224), 1169–1180, doi:10.3189/2014JoG13J230, 2014.
- Iglewicz, B. and Hoaglin, D.C.: How to detect and handle outliers (Vol. 16), Asq Press, 1993.
- Lomb, N.R.: Least-squares frequency analysis of unequally spaced data, *Astrophysics and space science*, 39(2), 447–462, doi:10.1007/BF00648343, 1976.
- Richter, A., Rysgaard, S., Dietrich, R., Mortensen, J. and Petersen, D.: Coastal tides in West Greenland derived from tide gauge records, *Ocean Dynamics*, 61(1), 39–49, doi:10.1007/s10236-010-0341-z, 2011.
- Scargle, J.D.: Studies in astronomical time series analysis, II-Statistical aspects of spectral analysis of unevenly spaced data, *The Astrophysical Journal*, 263, 835–853, doi: 10.1086/160554, 1982.
- Strozzi, T., Werner, C., Wiesmann, A. and Wegmuller, U.: Topography mapping with a portable real-aperture radar interferometer, *IEEE Geosci. Remote Sens. Lett.*, 9(2), 277–281, doi: 10.1109/LGRS.2011.2166751, 2012.
- Voytenko, D., Dixon, T.H., Howat, I.M., Gourmelen, N., Lembke, C., Werner, C.L., De La Peña, S. and Oddsson, B.: Multi-year observations of Breiðamerkurjökull, a marine-terminating glacier in southeastern Iceland, using terrestrial radar interferometry, *J. Glaciol.*, 61(225), 42–54, doi:10.3189/2015JoG14J099, 2015.
- Xie, S., Dixon, T.H., Voytenko, D., Holland, D.M., Holland, D. and Zheng, T.: Precursor motion to iceberg calving at Jakobshavn Isbræ, Greenland, observed with terrestrial radar interferometry, *J. Glaciol.*, 62(236), 1134–1142, doi:10.1017/jog.2016.104, 2016.

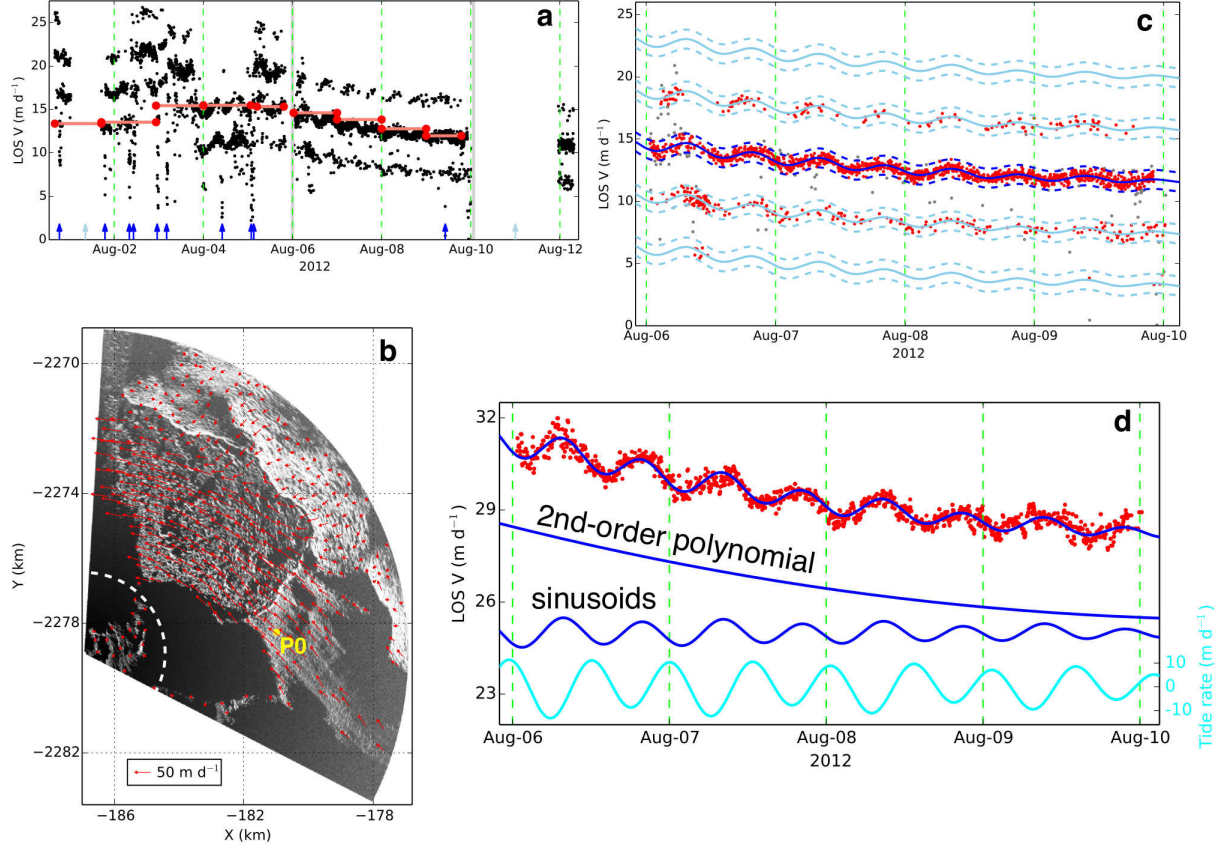


**Figure S1.** (a), LOS velocity time series (black dots) of P0 on (b), when using a stationary point on rock as reference for phase unwrapping. Pink bars show velocities by feature tracking method (shifted downwards by phase jumps of 4 cycles of radar wavelength), separated by  $\sim 1$  d. Blue arrows mark visible calving events on TRI intensity images, two light blue arrows represent calving events that were in observation gaps. (b), Point (P0) chosen as reference point for phase unwrapping to estimate relative velocities. Red arrows show 2-D velocity map by tracking two TRI intensity images between 00:01:00 7 August and 00:00:00 8 August. Background is a TRI intensity image acquired on 6 August 2012. Arrows within the dashed white arc are used to assess the uncertainty of feature tracking, the RMS is  $< 1$  m d<sup>-1</sup>. (c), LOS velocity time series between 6 August and 10 August (dots between two grey lines in (a)). Solid blue curve shows the best fit after “apparent outliers” (defined by modified Z-score method) removed, by using a 2nd-order polynomial plus 3 pairs of sinusoids model. Dashed blue curves show 3 times RMS space of the residuals. Solid and dashed Light blue curves are blue curves moved upwards/downwards by integer numbers of radar wavelength cycle. Dots fall into the  $3 \times$  RMS spaces (red) were used in (d), grey dots were removed as outliers. (d), Time series from (c) after shifting upwards by phase jump of 4 cycles of radar wavelength, and applying a median filter with a window-size of 3 (equals to 9 min in this case, where the repeating time of measurement is 3 min). Upper blue curve shows the best fitting by the same model as (c), but used filtered time series. Lower blue curves show the 2nd-order polynomial and sinusoids components, and are offset for clarity. Cyan curve shows local tidal height rate prediction.



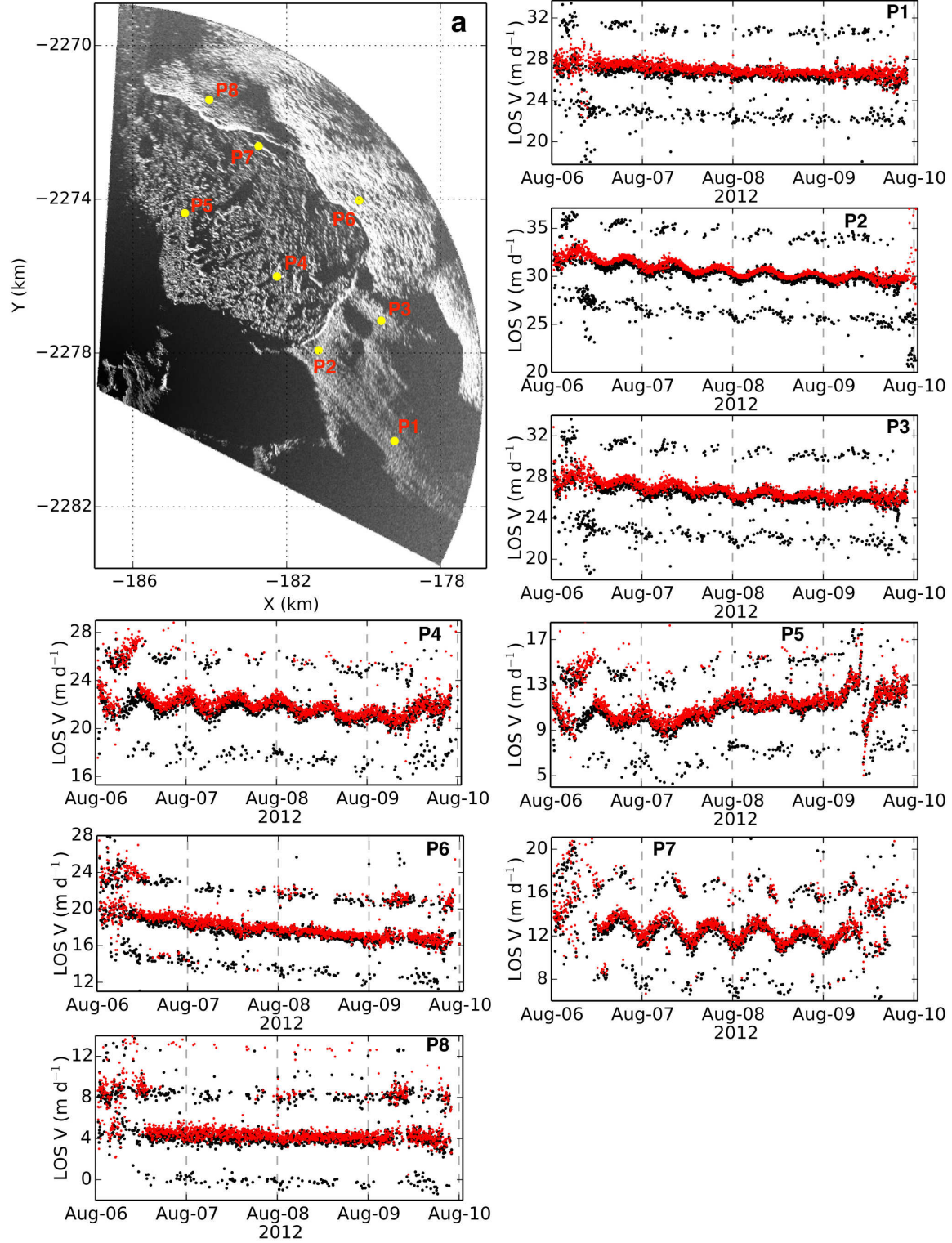


**Figure S2.** LOS velocities for selected points, after phase jumps fixed. (a), Point locations for P1 - P8. (P1-P8), Red dots are phase jumps fixed time series, black dots are time series when choosing a stationary point as reference for phase unwrapping, and were shifted upwards by 4 cycles of phase jumps.

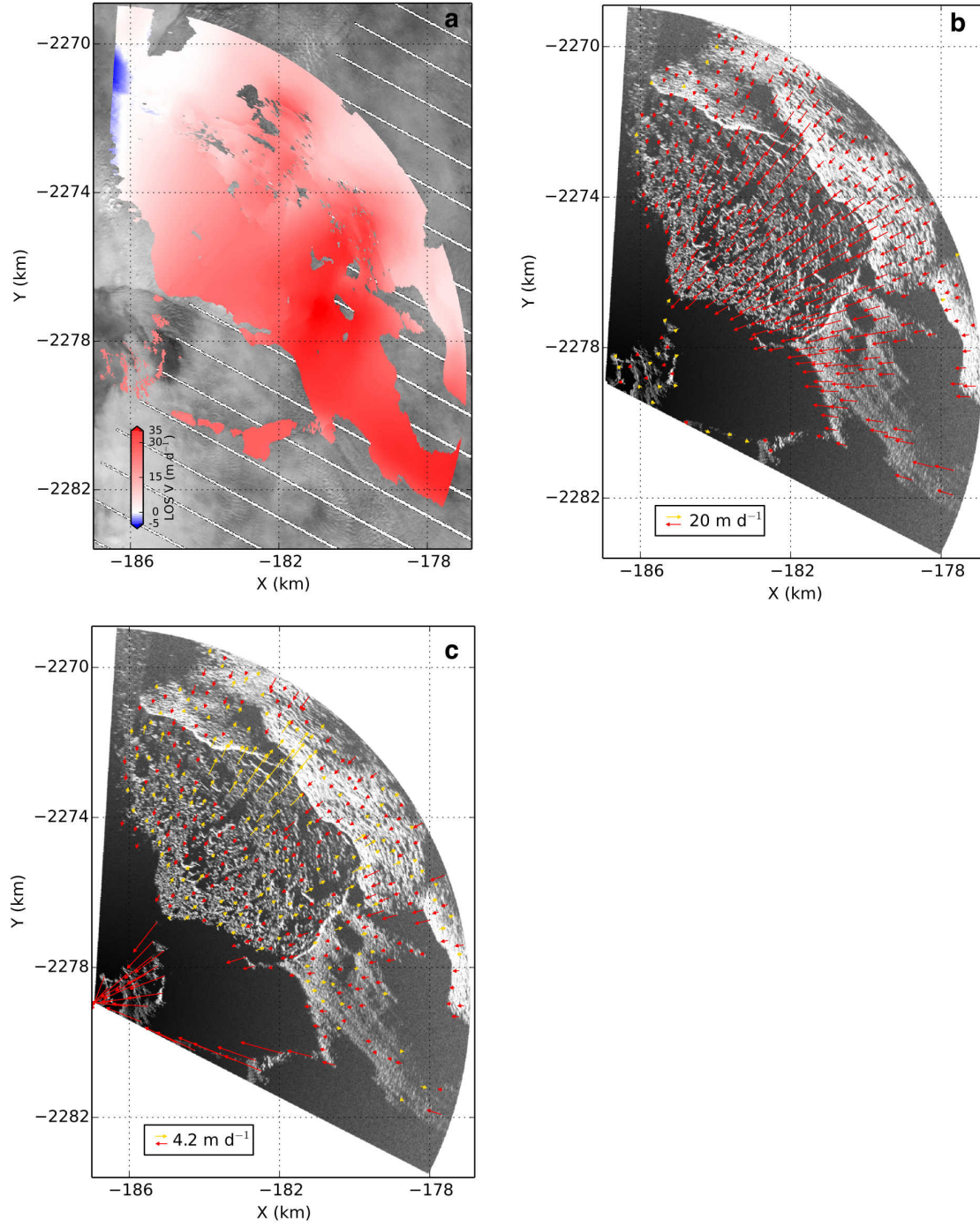


**Figure S3.** Comparison between velocity estimated by interferometry and feature tracking. (a), Median LOS velocity map by interferometry method for 7 August 2012, after phase jumps fixed. Background is a Landsat-7 image acquired on 6 August 2012, white stripes are data gaps. (b), Velocity map by feature tracking method, projected onto radar LOS direction. Red moves towards the radar, yellow away. (c), Difference between (a) and (b), red when velocity by interferometry is larger than by feature tracking, yellow vice versa. 4.2 m d<sup>-1</sup> equals to 1 cycle of phase jump.



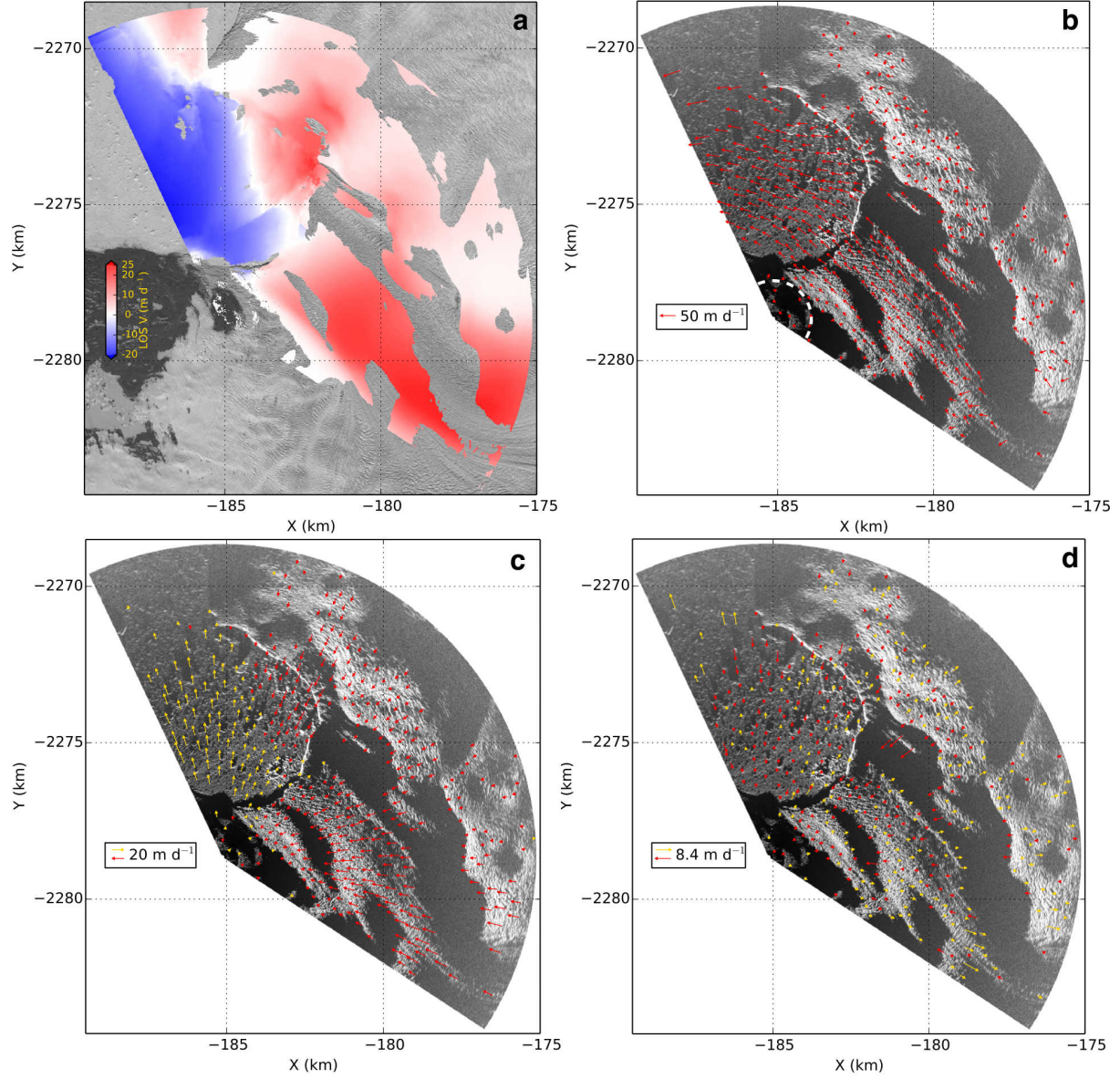


**Figure S4.** Comparison between velocity estimated by interferometry and feature tracking in 2015. (a), LOS velocity map by interferometry. (b), 2-D velocity map by feature tracking. Arrows within the dashed white arc are used to assess the uncertainty of feature tracking, the RMS is  $<1 \text{ m d}^{-1}$ . (c), Velocity map by feature tracking method, projected onto radar LOS direction. Red moves towards the radar, yellow away. (d), Difference between (a) and (c), red when velocity by interferometry is larger than by feature tracking, yellow vice versa.  $8.4 \text{ m d}^{-1}$  equals to 1 cycle of phase jump, when repeating time was 1.5 min.

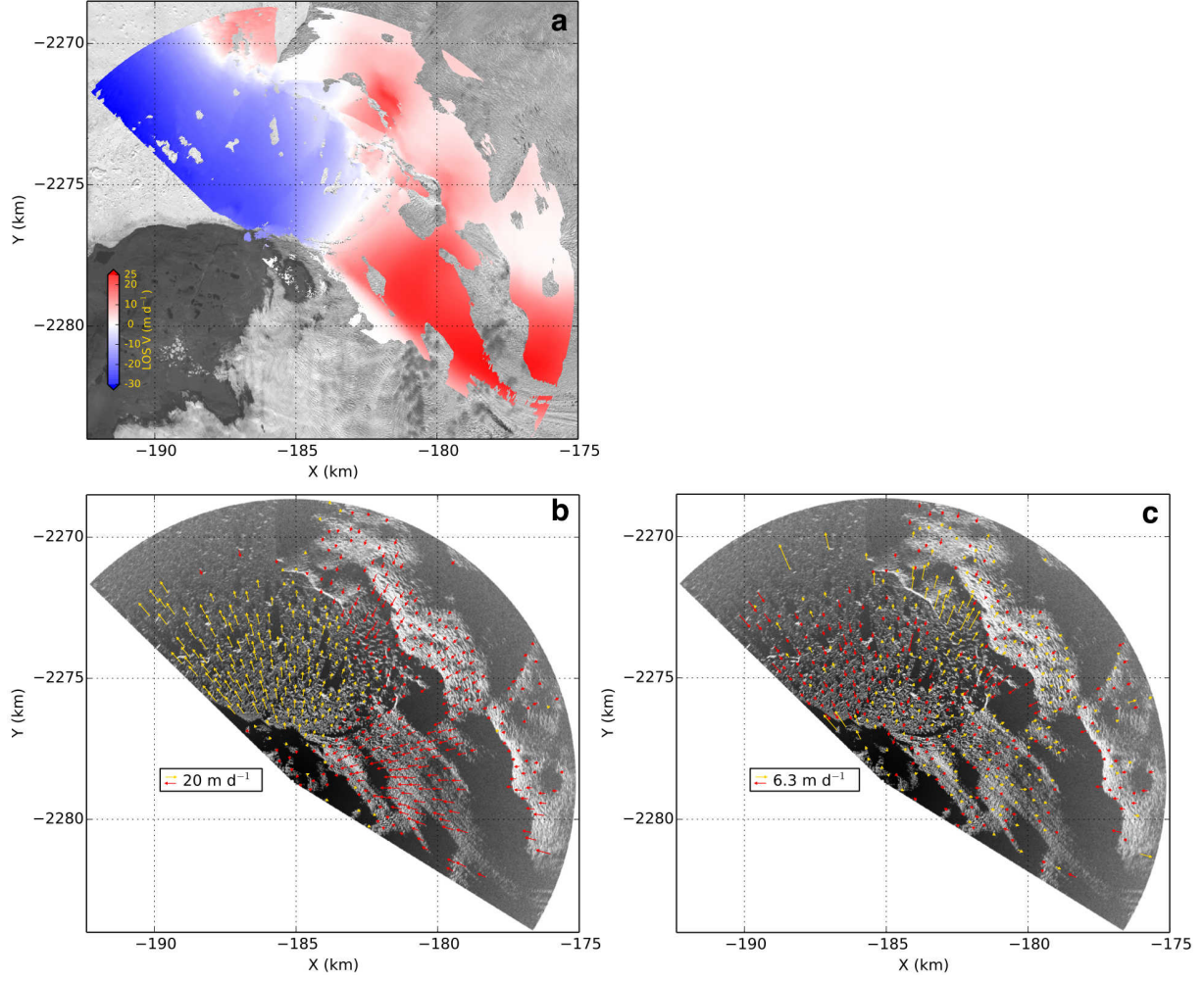


**Figure S5.** Comparison between velocity estimated by interferometry and feature tracking in 2016. Color and arrow denote the same as Fig. S3. In (c),  $6.3 \text{ m d}^{-1}$  equals to 1 cycle of phase jump, when repeating time was 2 min. The 2-D velocity map is shown in Fig. 3(a) of the main paper.

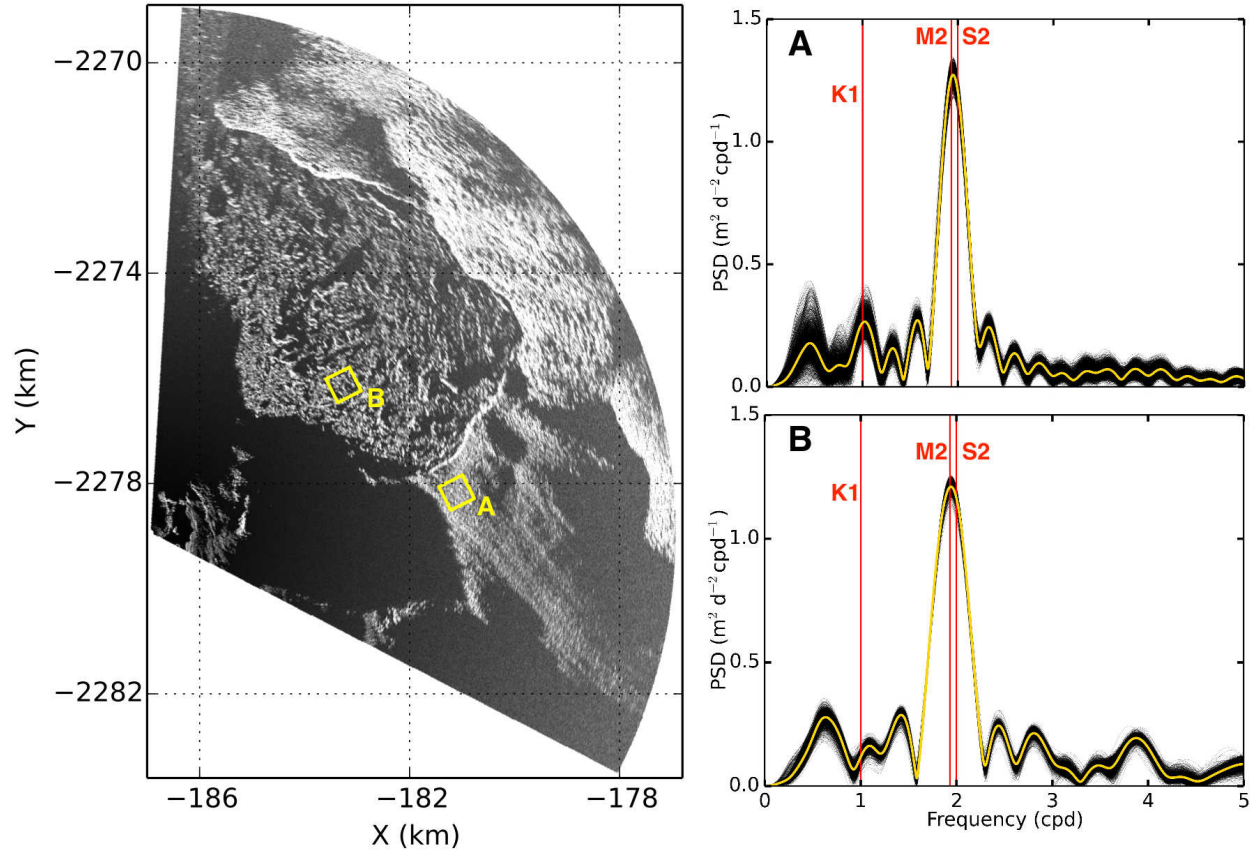


**Figure S6.** Stacked power spectral density (PSD) estimates of the LOS velocity time series for selected areas in 2012. Two  $0.5 \text{ km} \times 0.5 \text{ km}$  boxes (A and B) mark the selected areas. For PSD plots, each black line represents 1 pixel ( $10 \text{ m} \times 10 \text{ m}$ ) in the corresponding box. Yellow lines show the mean value. PSDs shown here are normalized. PSD analysis was done by using the Lomb-Scargle method (Lomb, 1976; Scargle, 1982). Red lines mark the frequencies of K1, M2, and S2 tide constituents.

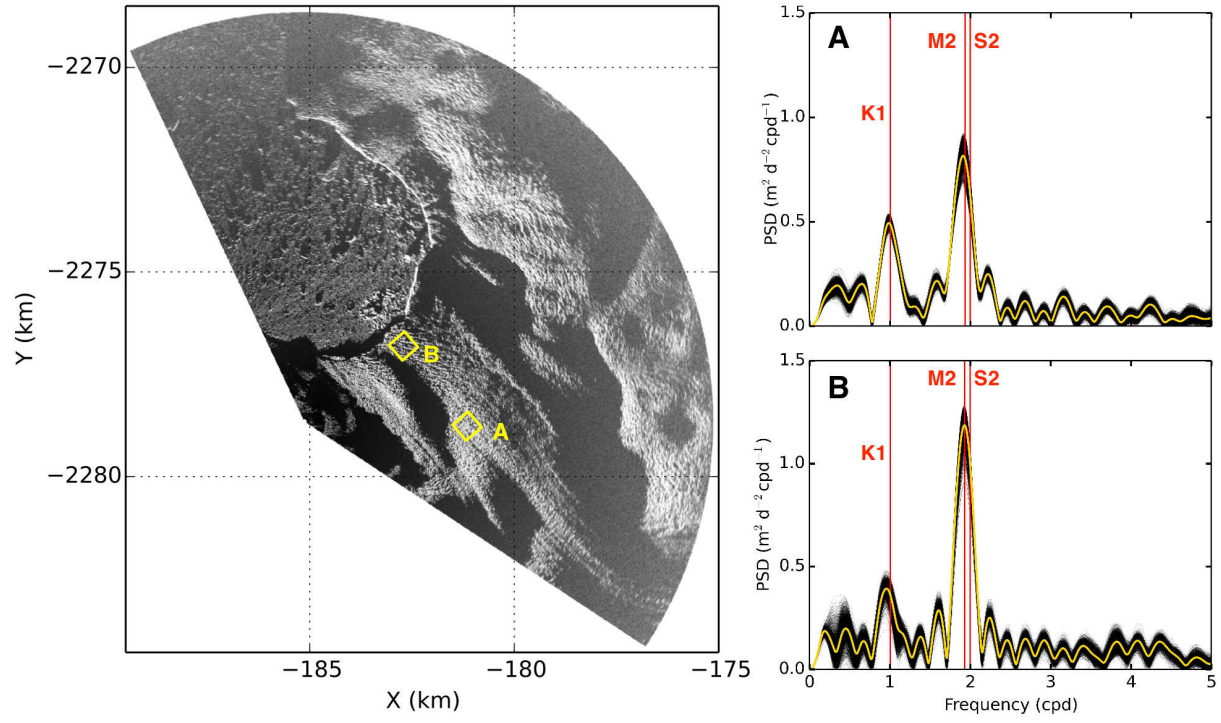


**Figure S7.** PSD plot for selected samples in 2015. Lines and colors denote the same as in Fig. S6.



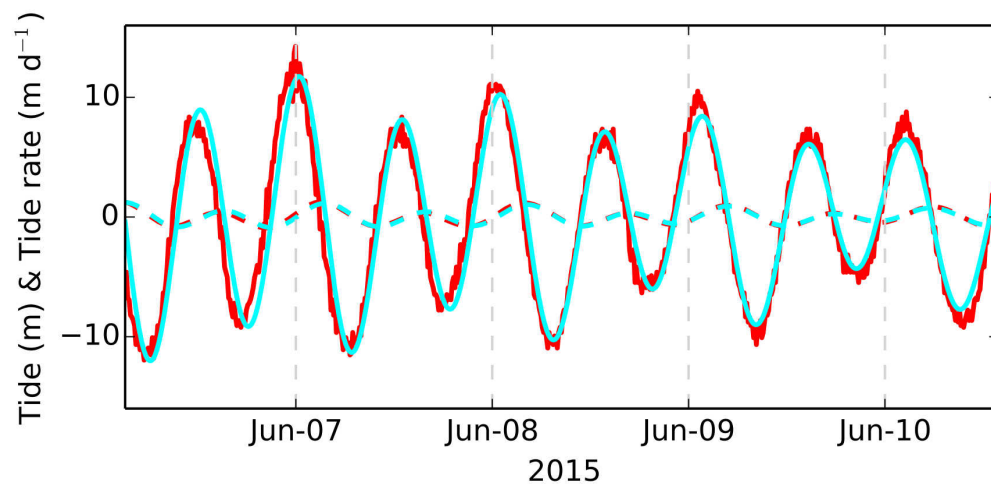


**Figure S8.** Predicted and observed tide and tidal rate during 2015 campaign. Tide is the dashed line, tidal rate is in solid line. Cyan color represents predicted tide and tidal rate, based on Richter et al. [2011]. Red color represents observed tide and derived tidal rate from a mooring at the mouth of the fjord.



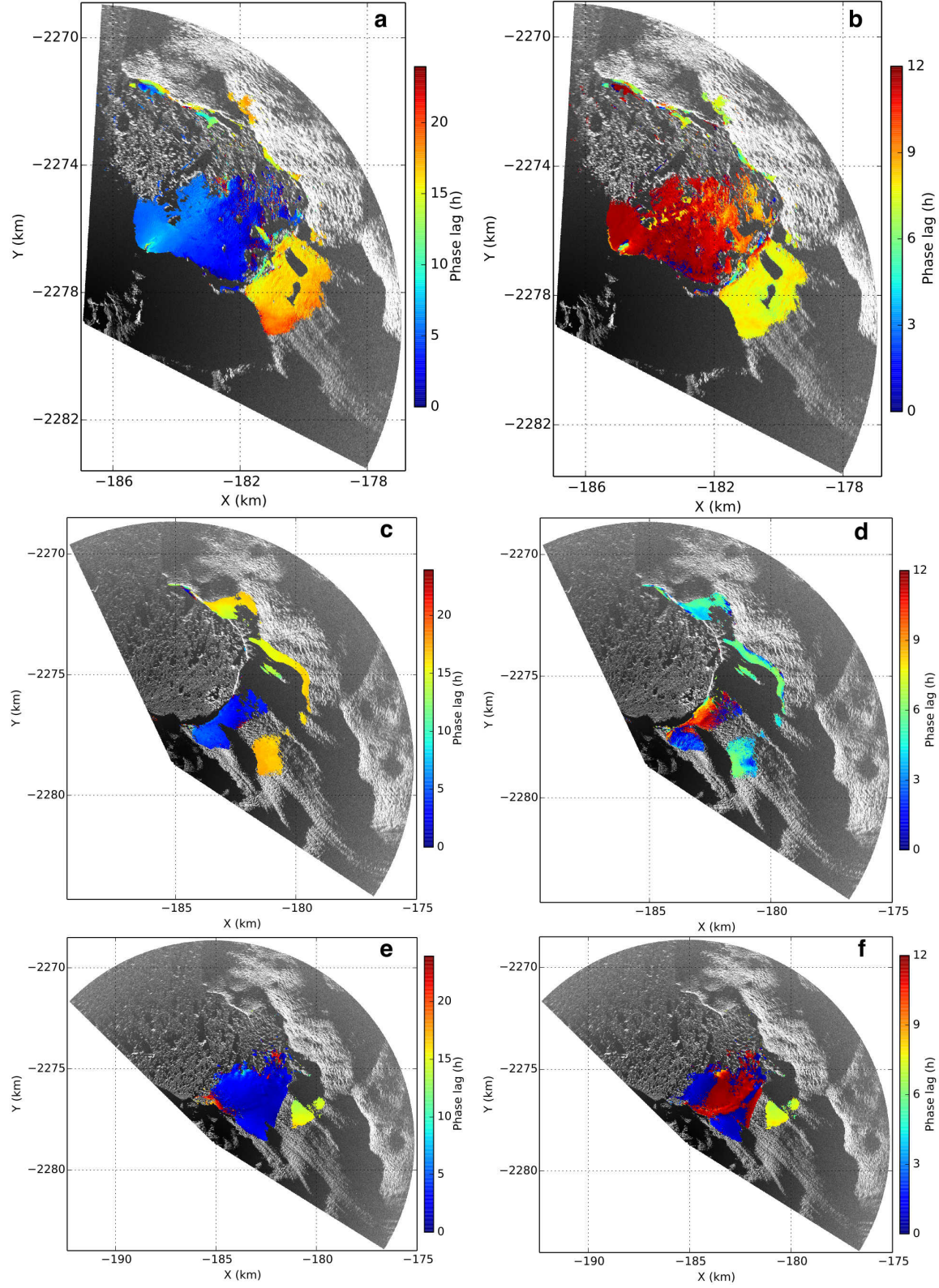


**Figure S9.** Phase lag maps of signals with K1 and S2 frequencies for each campaign. (a-b) for 2012, (c-d) for 2015, (e-f) for 2016. (a, c, e) show phase lags in time (h) for K1 frequency signal. (b, d, f) for S2 frequency signal. areas where SNR<1.5 are omitted.

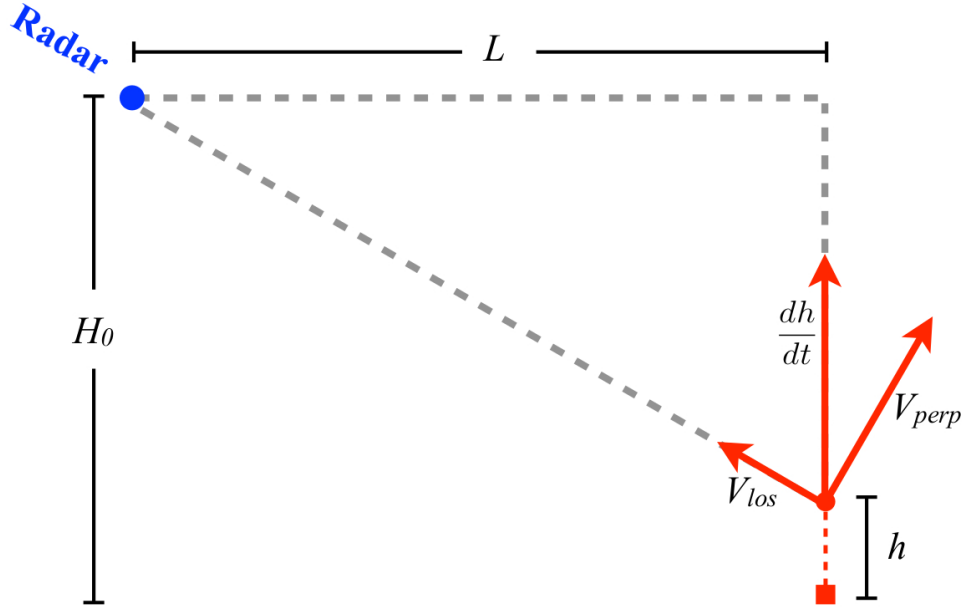


**Figure S10.** Geometry used to project velocity onto radar LOS direction. Blue dot represents the radar, red square shows the mean vertical position of the target, red dot is the vertical position at current time.  $H_0$  is the mean height difference between the radar and the target.  $L$  is the horizontal distance between the radar and the target.  $h$  is the vertical movement relative to  $H_0$ .  $dh/dt$  is the vertical component of ice velocity.  $V_{los}$  represents the TRI-observed LOS velocity.  $V_{perp}$  represents ice velocity projected onto perpendicular direction of the radar LOS.